Cell PRESS
Cancer Cell
Article

Colitis-Associated Colorectal Cancer Driven by T-bet Deficiency in Dendritic Cells

Wendy S. Garrett,[1,2,4,*] Shivesh Punit,[1,5] Carey A. Gallini,[1] Monia Michaud,[1] Dorothy Zhang,[1] Kirsten S. Sigrist,[1] Graham M. Lord,[1,6] Jonathan N. Glickman,[3,7] and Laurie H. Glimcher[1,2,*]
[1]Department of Immunology and Infectious Diseases, Harvard School of Public Health, Boston, MA 02115, USA
[2]Department of Medicine
[3]Department of Pathology, Brigham and Women's Hospital
Harvard Medical School, Boston, MA 02115, USA
[4]Department of Medical Oncology, Dana Farber Cancer Institute, Boston, MA 02115, USA
[5]Present address: Department of Cell and Developmental Biology, Vanderbilt University, Nashville, TN 37240, USA
[6]Present address: Department of Nephrology and Transplantation, King's College London and Guy's and St. Thomas' Hospital, London SE1 9RT, UK
[7]Present address: GI Pathology, Boston Caris Diagnostics, 320 Needham Street, Suite 200, Newton, MA 02464, USA
*Correspondence: wendy_garrett@dfci.harvard.edu (W.S.G.), lglimche@hsph.harvard.edu (L.H.G.)
DOI 10.1016/j.ccr.2009.07.015

SUMMARY

We previously described a mouse model of ulcerative colitis linked to T-bet deficiency in the innate immune system. Here, we report that the majority of *T-bet*$^{-/-}$ *RAG2*$^{-/-}$ ulcerative colitis (TRUC) mice spontaneously progress to colonic dysplasia and rectal adenocarcinoma solely as a consequence of *MyD88*-independent intestinal inflammation. Dendritic cells (DCs) are necessary cellular effectors for a proinflammatory program that is carcinogenic. Whereas these malignancies arise in the setting of a complex inflammatory environment, restoration of *T-bet* selectively in DCs was sufficient to reduce colonic inflammation and prevent the development of neoplasia. TRUC colitis-associated colorectal cancer resembles the human disease and provides ample opportunity to probe how inflammation drives colorectal cancer development and to test preventative and therapeutic strategies preclinically.

INTRODUCTION

The three highest risk groups for developing colorectal cancer (CRC) are individuals with ulcerative colitis (UC), familial adenomatous polyposis, and hereditary nonpolyposis colon cancer syndrome. Among UC patients, the relative risk of developing CRC correlates with the extent and duration of disease—18% will have developed CRC after 30 years of disease (Eaden et al., 2001; Xie and Itzkowitz, 2008). The sequence of genetic events in colitis-associated CRC (caCRC) differs from that observed in sporadic CRC. In caCRC, chromosomal instability (CIN) and DNA damage can precede and predict the development of dysplasia, and alterations in *p53* expression occur early in the oncogenic pathway, not as is depicted in the classic adenoma-carcinoma sequence (Cho and Vogelstein, 1992; Clausen et al., 2001; Itzkowitz, 2003; Yoshida et al., 2003). In addition, in contrast to sporadic CRC, alterations in β-catenin localization reflecting *APC* mutations occur very late in the caCRC transformation process. Sporadic CRC carcinogenesis is typified by the transformation of the adenoma to an adenocarcinoma (ACA); however, in caCRC, invasive carcinomas frequently arise in flat areas of dysplasia. This feature of caCRC makes clinical surveillance of this at risk population particularly challenging and speaks to the distinct biology of these neoplasias.

Mouse models of intestinal cancer have been instrumental in understanding oncogenesis and have shed light on the role of

SIGNIFICANCE

Inflammatory bowel disease (IBD) is one of the three highest risk factors for colorectal cancer (CRC). The molecular pathogenesis of IBD-associated colorectal cancer (caCRC) differs from that of sporadic CRC. The findings reported here demonstrate that the *T-bet*$^{-/-}$ *RAG2*$^{-/-}$ ulcerative colitis model of caCRC is a robust system for studying the human disease. This model establishes the importance of the innate immune system and specifically dendritic cells as key cellular effectors in inflammation that drives neoplasia. Our data also demonstrate that there are *MyD88*-independent pathways to caCRC. Finally, the observation that overexpression of *T-bet* in innate immune cells prevents caCRC provides an additional explanation for why colorectal cancer patients with intratumoral *T-bet* expression may have improved survival and generates interest in immune-based cancer therapeutics.

innate immunity and the commensal microbiota in colon cancer. We recently described a model of commensal-dependent UC termed *T-bet*$^{-/-}$ *RAG2*$^{-/-}$ UC (TRUC) that results from T-bet deficiency in the innate immune system (Garrett et al., 2007). *T-bet* is a T-box family transcription factor that controls chemokine, chemokine receptor, and cytokine expression; regulates host-commensal homeostasis in the colon; and is expressed only in immune cells (Glimcher, 2007; Ma, 2007). TRUC mice develop a severe and highly penetrant colitis, driven in part by loss of *TNF-α* regulation in the colon, that can be reversed by antibiotics, TNF-α blockers, or transfer of T regulatory cells. CRC has been documented in other inflammatory bowel disease (IBD) mouse models including *IL-10*$^{-/-}$, *TCRα*$^{-/-}$, *Gαi2*$^{-/-}$, *IL-2*$^{-/-}$ × *β2m*$^{-/-}$, and *αv*$^{-/-}$ mice (Berg et al., 1996; Dianda et al., 1997; Lacy-Hulbert et al., 2007; Rudolph et al., 1995; Shah et al., 1998). This observation coupled with the finding that increased levels of T-bet in human colorectal tumors correlate with increased patient survival spurred us to determine if TRUC mice, whose colitis is mechanistically distinct from other IBD models, would develop caCRC (Pages et al., 2005).

RESULTS

TRUC Mice Develop Dysplasia and Carcinoma Resembling Human IBD-Associated CRC

In our colony, TRUC manifests a juvenile colitis that starts rectally, has 100% penetrance, and can result in bacteremia and death as early as 10 weeks of age. We monitored large cohorts (>400 TRUC mice during a 3 year period) to robustly survey whether dysplasia and carcinoma would develop over time. At 3 months of age, 50% of TRUC mice had dysplastic lesions and ACA was present in 3/40 cases. By 6 months of age, over 96% of mice had dysplastic lesions and 42% had ACA (Figure 1A). Low-grade dysplasia (LGD) predominated in younger mice (75% of cases), while 6 month olds manifested high-grade dysplasia (HGD) (89% of cases) (Figure 1B). In 12/30 of the HGD cases there were adjacent regions of LGD (1–3 mm) (data not shown), suggesting progression to the higher grade. Similarly, ACA (size range 2–7 mm) were flat and usually arose in the rectum within regions of dysplastic mucosa (25/31 cases), similar to what is observed in UC patients. The number of mice with more advanced submucosal invasive cancers increased over time (Figure 1C). Hence, malignant transformation of intestinal epithelial cells occurs in virtually all TRUC mice by 6 months of age and progresses to frank ACA in a significant proportion of animals.

On gross examination, areas of colitis with dysplasia and ACA appeared more vascular and engorged as compared with colons with similar inflammatory scores but no dysplasia or cancer (Figure 1D). We noted the occurrence of fixed anorectal prolapse as it can complicate the diagnosis of cancer and dysplasia (10/21 intramucosal and 2/10 submucosal ACA cases). Photomicrographs are shown from representative cases with carcinoma (Figure 1E, upper panel; dysplasia [middle panel: left, HGD; right, LGD], and no dysplasia [bottom panel: left, colitis; right, no colitis]).

Immunohistochemistry for PCNA revealed a high degree of proliferation in mice with ACA and dysplasia, consistent with neoplastic transformation (Figure 1F, upper left panel). To determine whether TRUC caCRC phenotypically resembled human caCRC, we assessed the expression of additional markers by immunohistochemistry. Similar to human caCRC, and in contrast to what is observed in sporadic CRC, β-catenin localization was membranous in nondysplastic and dysplastic lesions (Figure 1F, upper right panel) and nuclear (indicative of APC loss of function) in carcinoma (Figure 1F, upper right panel). As is observed in human caCRC, we saw high levels of epithelial cell and immune cell COX-2 expression in inflamed mucosa that was nonneoplastic and neoplastic (Figure 1F, middle panel) (Agoff et al., 2000). Approximately 30% of nonneoplastic crypts were positive for COX-2 and >90% of neoplastic crypts were positive (Figure 1F, middle panel); thus *COX-2* epithelial expression is a premalignant feature of TRUC transformation. Intense nuclear staining for p53 (CM5 clone: detects both mutant and wild-type forms) was detected in the neoplastic epithelium and in nondysplastic crypts; an observation that is highly suggestive of *p53* mutations (Rodrigues et al., 1990) (Figure 1F, bottom panel). To assess if this increased *p53* expression was a consequence of mutations resulting in loss of p53 function, we performed two complementary experiments examining both the DNA binding capability of p53 and induction of p53 target genes. Specifically, we tested p53 DNA binding activity and expression of the p53 target genes, *p21* and *APAF1*, in colonic epithelial cells (CECs) from control, nonneoplastic TRUC, and neoplastic TRUC in response to treatment with doxorubicin, an anthracycline chemotherapeutic that inhibits topoisomerase II, induces double-stranded DNA breaks, and strongly activates *p53* (Ravizza et al., 2004). Doxorubicin treatment induced p53 binding to a consensus site oligonucleotide in *RAG2*$^{-/-}$ (control) CECs in a specific fashion but was reduced in TRUC nonneoplastic CECs and markedly diminished in neoplastic TRUC CECs (Figure 1G, upper panel). *p21* expression was induced approximately 250-fold in *RAG2*$^{-/-}$ CECs treated with doxorubicin; however, this induction was more modest in TRUC nonneoplastic CECs (70.2-fold) and substantially reduced in neoplastic TRUC CECs (2.23-fold) (Figure 1G, lower left panel). APAF1 levels in response to doxorubicin were upregulated most in *RAG2*$^{-/-}$ (1321-fold), approximately an order of magnitude less in TRUC nonneoplastic (100.3-fold) and substantially reduced in TRUC neoplastic (1.42-fold) samples (Figure 1G, lower right panel). Thus the TRUC neoplastic process does resemble human caCRC in several aspects of its molecular pathogenesis, specifically in both early loss of function of *p53* and increased epithelial *COX-2* expression and later *APC* mutations.

TRUC Mice Develop Colonic Epithelial Aneuploidy prior to Dysplasia, and the TRUC Mucosa Is Rich in ROS, Colonic Epithelial DNA Adducts, and Cytokines, Similar to IBD Patients Who Develop Dysplasia and Cancer

CIN and its resulting aneuploid DNA content are features of human caCRC. In fact, CIN has been detected in UC patient colonic biopsies that are nondysplastic, dysplastic, and malignant; and aneuploidy predicts dysplasia (Clausen et al., 2001; Meling et al., 1991a, 1991b; Rubin et al., 1992). To search for CIN and aneuploidy in TRUC mice with and without dysplasia and cancer, we measured DNA content in CECs from TRUC colons by flow cytometry. While no aneuploid cell populations were detected in 6 month old *RAG2*$^{-/-}$ mice (data not shown), aneuploidy was a feature of nondysplastic and dysplastic

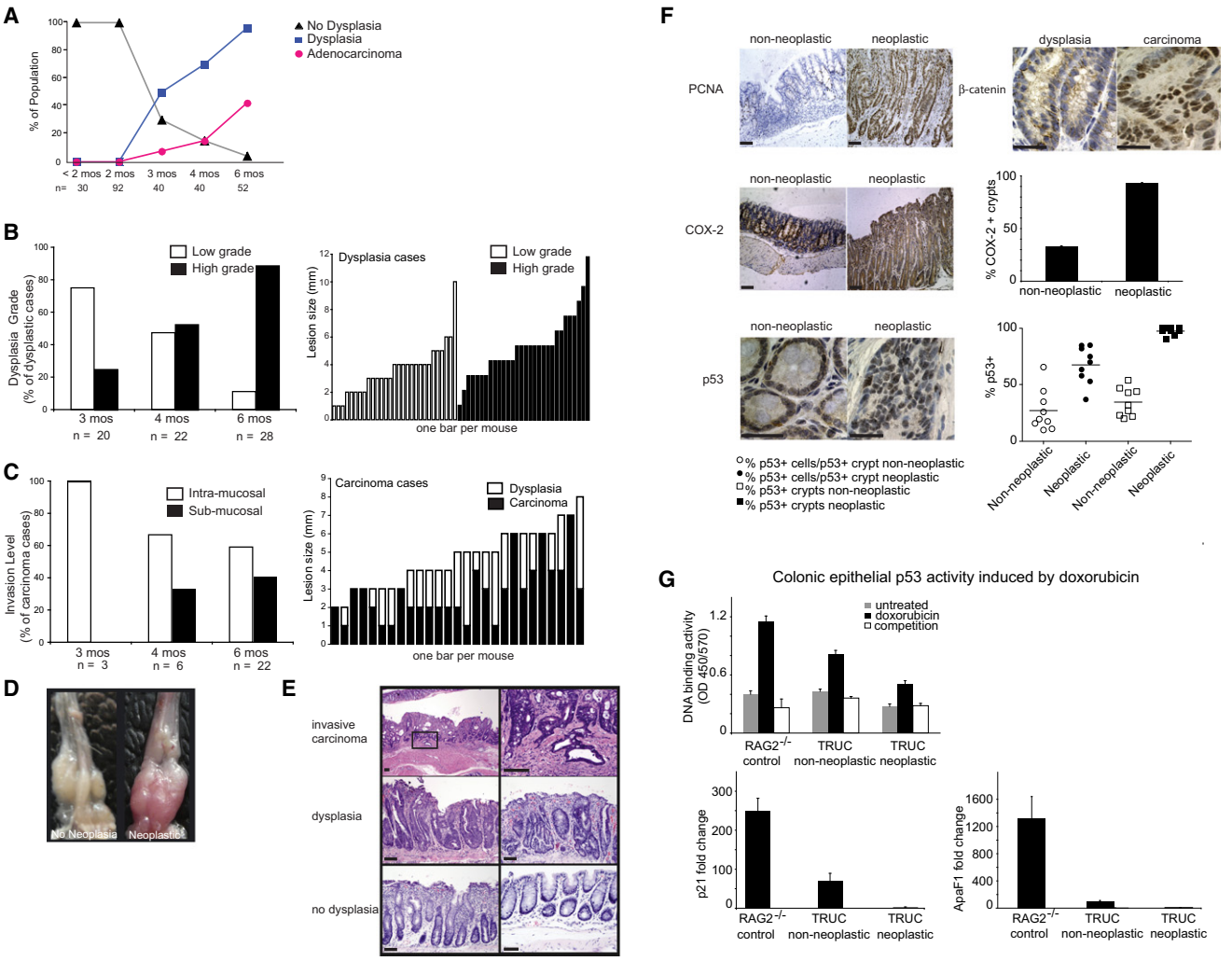

Figure 1. TRUC Mice Develop caCRC

(A) Percentage of TRUC mice with and without dysplasia and cancer is shown as a function of mouse age (in months). The number of mice surveyed is displayed along the x axis. No cancers were observed in age-matched *RAG2*$^{-/-}$ (data not shown).

(B) Dysplastic grade is shown as a percentage of dysplastic cases for mice at 3, 4, and 6 months. Size (mm) of low- and high-grade dysplastic lesions is displayed for each animal.

(C) Level of invasion (intramucosal versus submucosal) is shown as a percentage of carcinoma cases. Lesion size (mm) of the carcinomas (shaded bars) and continuous areas of dysplasia (open bars) are plotted for individual cases.

(D) Photographs of TRUC colons with colitis but no dysplasia (left) and with CRC (right).

(E) Histology from TRUC mice with invasive carcinoma (upper panel), dysplasia (middle panel [left: HGD, right: LGD]), and no dysplasia (lower panel [left: colitis, no dysplasia, right: no colitis, no dysplasia]). Scale bars, 100 μm.

(F) Immunohistochemistry. (left upper panel) PCNA. Scale bars, 100 μm. (right upper panel) β-Catenin staining in dysplastic epithelial crypts (left) and nuclear staining in invasive carcinoma (right). Scale bars, 25 μm. COX-2 (left middle panel) and quantitation of COX-2+ crypts (right middle panel). Scale bars, 100 μm. P53 (left lower panel, nuclear staining in crypts) and quantitation of p53 staining (right lower panel); each dot represents data from one mouse. Scale bars, 25 μm.

(G) Colonic epithelial p53 activity induced by doxorubicin. (left upper panel) Consensus oligonucleotide binding activity of p53 in nuclear extracts of CECs from *RAG2*$^{-/-}$ versus TRUC nonneoplastic versus TRUC neoplastic colons. Gray bars are from untreated samples, black bars are from doxorubicin-treated CECs incubated with biotinylated oligonucleotides, and open bars are from doxorubicin-treated CECs incubated with biotinylated and 20-fold excess unbiotinylated oligonucleotides. Data represent the mean of two independent experiments with primary epithelial cells pooled from 20 mice per group (*RAG2*$^{-/-}$, TRUC non-neoplastic, and TRUC neoplastic). Error bars denote ± SD. (left lower panel) *p21* induction in response to doxorubicin. Real-time qPCR was performed on control and doxorubicin-treated samples. Fold change between doxorubicin and untreated samples was calculated by dividing their respective $2^{-\Delta Ct}$ values. (right lower panel) *APAF1* induction in response to doxorubicin was determined on the same sample set as above. Bars represent the mean of two independent experiments and error bars the ± SD.

TRUC colons and was most pronounced in those with dysplasia and cancer (mean 2.34% [nonneoplastic] versus 6.11% [neoplastic], p = 0.0005) (Figure 2A).

Although the exact mechanisms by which inflammation drives CIN remain controversial, there is more consensus regarding how other types of DNA damage, e.g., DNA adducts, occur in

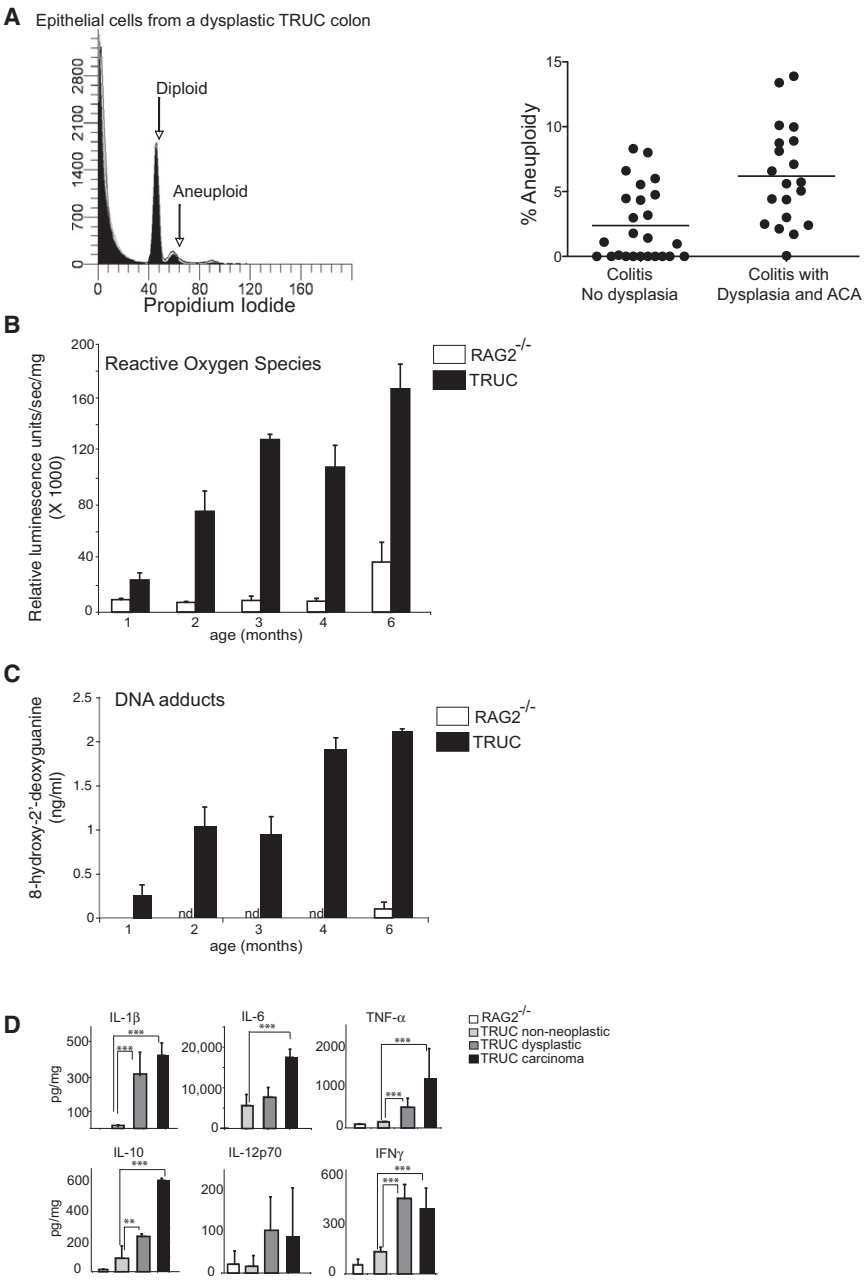

Figure 2. Chromosomal Instability and Reactive Oxygen Induced DNA Adducts in TRUC Carcinogenesis

(A) Flow cytometric aneuploidy analysis of epithelial cells isolated from mice without dysplasia, with dysplasia, and with carcinoma. (left panel) Representative plot from one mouse with diploid and aneuploid populations labeled. (right panel) Percentage of aneuploid epithelial cells for all mice analyzed. Each dot represents data from one mouse. Horizontal bars represent the mean.

(B) ROS were measured in TRUC versus *RAG2*$^{-/-}$ distal colons. Reactive luminescence measured in units/second/milligram of colonic tissue × 1000 (y axis) is plotted as a function of mouse age. Open bars show *RAG2*$^{-/-}$ and shaded bars show TRUC (five to eight mice per group). Means are graphed; error bars represent ± SD, $p < 0.001$ for all comparison between TRUC 1 month and TRUC 2–6 months.

(C) 8′hydroxy-2′deoxyguanine (ng/ml) levels in CECs. *RAG2*$^{-/-}$ control (age 1 and 6 months, open bars, n.d. = not performed for *RAG2*$^{-/-}$ [age 2–4 months]) and TRUC mice (age 1–6 months, shaded bars). Six to nine mice were used per time point. Means are graphed; error bars represent ± SD, $p < 0.001$ for all comparison between TRUC 1 month and TRUC 2–6 months.

(D) ELISA-based protein determinations for selected cytokines are shown from explant cultures pooled from five to seven specimens per time point from *RAG2*$^{-/-}$ versus TRUC colitic (nonneoplastic) versus TRUC dysplastic versus TRUC carcinoma. Bars represent the mean values for three independent sets of pooled samples and error bars represent ± SD.

the setting of inflammation. Reactive oxygen species (ROS) and other oxidative stressors drive DNA damage by oxidizing DNA bases and generating DNA adducts at a rate that outpaces DNA repair mechanisms. ROS and DNA adducts have been well characterized in IBD patients and in animal models of intestinal inflammation (D'Inca et al., 2004). We found that the TRUC inflammatory milieu was rich in ROS and that increased ROS levels correlated with TRUC carcinogenesis (Figure 2B). To determine if DNA adducts were an untoward consequence of ROS we measured levels of 8-hydroxy-2-deoxyguanine in TRUC CECs. We found that DNA adducts were detectable in young TRUC and aged *RAG2*$^{-/-}$ mice; however, the levels of these adducts increased 3-fold between 1 and 2 months in TRUC mice and were highest in 4 and 6 month old TRUC mice (enriched for dysplasia and carcinoma) ($p < 0.001$, for all TRUC comparisons 1 month versus 2–6 months) (Figure 2C). The inflammatory microenvironment was rich in several cytokines (e.g., IL-1β, TNF-α, IL-6, IFNγ, and IL-10), many of which increased in colonic explant cultures with dysplasia and carcinoma (Figure 2D). We have examined the expression of a number of cytokines, proinflammatory mediators, growth factors, and proteases and found that the vast majority increased in the transition from colitis to dysplasia and colitis to carcinoma (see Figures S1A and S1B available online). Thus the chronically inflamed TRUC mucosa is a prooncogenic environment rich in ROS, DNA adducts, as well as numerous cytokines and growth factors with mitogenic potential.

Unbalanced Epithelial Cell Death and Proliferation in TRUC Mice

At its core this upregulation of cytokines, proteases, and growth factors represents a repair response; however, in the setting of ROS and CIN a prooncogenic environment is the result. We investigated the response of the epithelium to this environment by carefully interrogating epithelial cell proliferation and cell

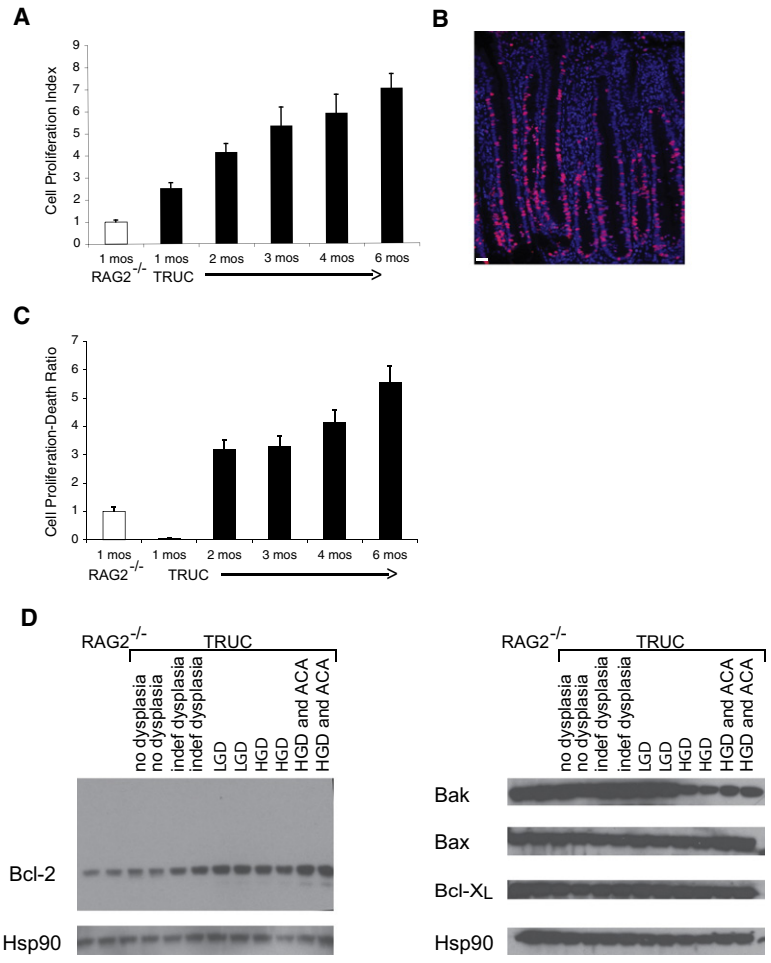

Figure 3. Imbalance between Cell Death and Proliferative Repair in TRUC Mice

(A) The TRUC epithelium is highly proliferative and epithelial proliferation increases with time. Cell proliferation index (BrDU+ cells/[epithelial cells/crypt]) normalized to *RAG2*$^{-/-}$ levels is plotted along the y axis. The mean of six *RAG2*$^{-/-}$ (age 1 month) and five to seven TRUC per time point (age 1–6 months) is shown; error bars represent ± SD.

(B) Representative immunofluorescence micrograph of data quantitated in (A) showing a hyperproliferative TRUC mucosa with BrDU staining (red) and DAPI-labeled nuclei (blue). Scale bar, 25 μm.

(C) Cell proliferation outpaces cell death as TRUC mice age. Sections from the mice in (A) were stained with the TUNEL reagent to label dying epithelial cells. The number of TUNEL+ epithelial cells/(epithelial cells/crypt) was then divided by the Cell Proliferation Index. This ratio normalized to the calculated value observed for the *RAG2*$^{-/-}$ samples is plotted along the y axis. The mean value for six *RAG2*$^{-/-}$ (age 1 month) and five to seven TRUC per time point (age 1–6 months) is shown; error bars represent ± SD.

(D) Epithelial cell lysates were generated from distal CECs from TRUC and *RAG2*$^{-/-}$. Each lane represents sample from two mice, and two separate groups with the indicated pathology were examined by western blot for Bcl-2, Bak, Bax, and Bcl-xL levels. Hsp 90 was used as a loading control.

death. We found that the TRUC epithelium became increasingly hyperproliferative with time (Figures 3A and 3B). Furthermore, quantifying cell death in the epithelium by TUNEL staining and proliferation by BrDU staining revealed marked imbalances between cell death and proliferation in the TRUC epithelium. At 4 weeks of age, cell death outpaced the proliferative response. However, once initiated, the repair response surpassed a homeostatic level of epithelial maintenance, even considering the increase in regenerative activity secondary to colitis (Figure 3C). It was possible that the TRUC inflammatory milieu also altered the balance of apoptotic and antiapoptotic proteins in the epithelium as evidenced by imbalances in the expression of proteins regulating apoptosis and hyperproliferation. Western blot analysis of *Bcl-2* family members in CEC extracts from TRUC samples across the neoplastic continuum and from *RAG2*$^{-/-}$ samples revealed increased antiapoptotic Bcl-2 in dysplastic samples versus nondysplastic samples and decreased proapoptotic Bak in samples with HGD and cancer (Figure 3D). Alterations in Bcl-2 and Bak levels accompany the hyperproliferation and decreased cell death observed during TRUC neoplastic transformation. The ROS of the inflammatory environment may exert selective pressure on the epithelium and epithelial cells with reduced apoptotic potential, due to increased Bcl-2 and decreased Bak, may have a survival advantage.

TRUC Colonic Neoplasia Is Dependent on an Inflammatory Response to Commensal Bacteria that Is *MyD88* Independent and Can Be Blunted by Early, but Not Late, TNF-α Neutralization

The profound effects on proliferation and apoptosis observed in TRUC epithelium amidst the complexity of the TRUC inflammatory milieu suggested that treatment of the underlying inflammation might alter the development of dysplasia and cancer. We had previously shown that broad-spectrum antibiotic treatment ameliorated TRUC colitis by changing but not eliminating the commensal microflora. To determine if altering the commensal microflora would reduce the incidence of TRUC neoplasia, we undertook a long-term course (6 months) of continuous antibiotic treatment over the time period during which TRUC mice develop dysplasia and cancer. None of the mice in the antibiotic treatment group developed colitis (Figure 4A, left panel), but 100% of the mice in the control group had very severe colitis by 6 months of age. In contrast to the control group, which showed HGD (40% of cases) and ACA (60% of cases), none of the antibiotic-treated mice had neoplasia (Figure 4A, right panel). These data suggest that neoplasia in TRUC mice is dependent on an inflammatory response that in turn requires the presence of the full complement of the TRUC commensal microflora.

Typically, the innate immune system senses microbes via microbial pattern-recognition receptors, of which the Toll-like receptors (TLRs) are one major family of these. TLRs have emerged as negative regulators of cancer and TLR stimulation is now recognized as a driver of tumorigenesis (Rakoff-Nahoum and Medzhitov, 2009). Therefore, we tested whether loss of *MyD88*, a crucial TLR signaling molecule, would affect TRUC colitis and caCRC as has been shown in the *IL-10*$^{-/-}$ colitis

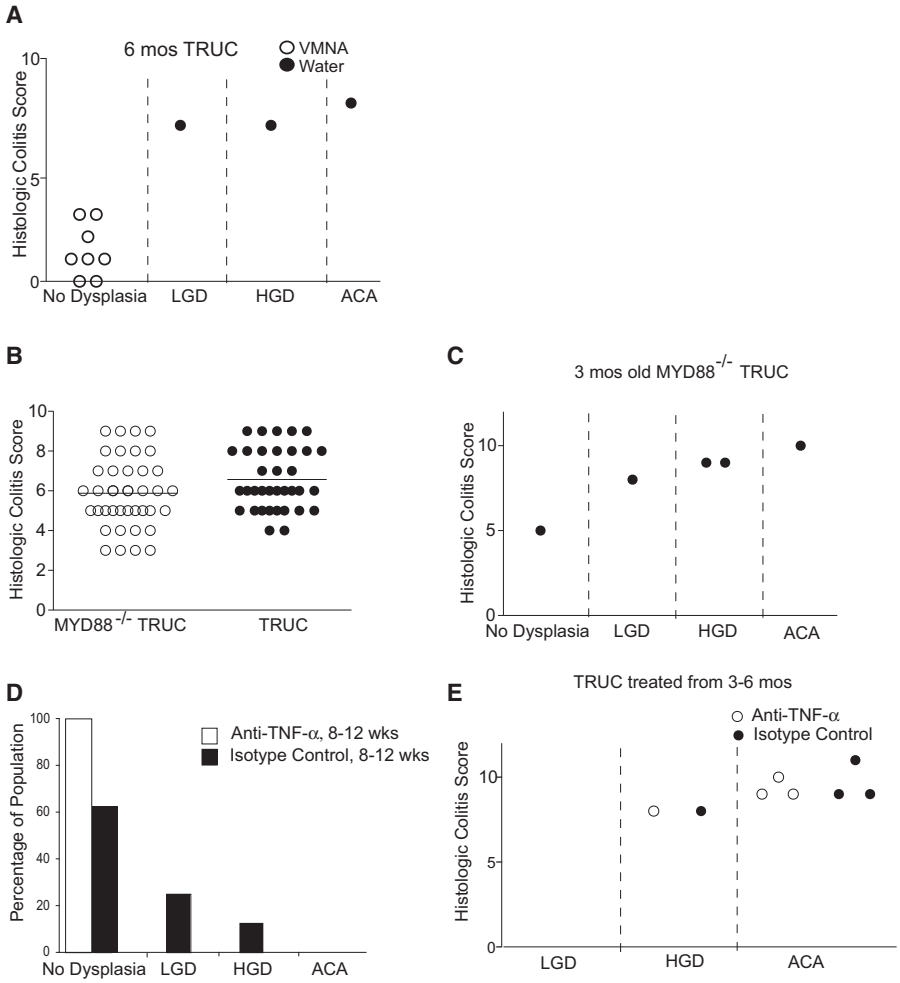

Figure 4. TRUC Colonic Neoplasia Is Dependent on an Inflammatory Response to Commensal Bacteria that Is *MyD88* Independent and Can Be Blunted by Early, but not Late, TNF-α Neutralization

(A) Six-month-old TRUC mice treated with continuous broad spectrum antibiotics do not develop neoplasia. Histologic colitis score (y axis) and neoplastic classification (x axis) (LGD, HGD, and ACA). Vancomycin, metronidazole, neomycin, and ampicillin treated (open circles) and water control (shaded circles).

(B) *MyD88*$^{-/-}$ TRUC develop colitis and neoplasia. (left) Histologic colitis scores for 8 week old *MyD88*$^{-/-}$ TRUC (open circles) and TRUC (shaded circles). (right) Histologic colitis scores (*y* axis) and distribution of the degree of neoplasia (x axis) for 12 week old *MyD88*$^{-/-}$ TRUC.

(C) Mice treated with anti-TNF-α from 8–12 weeks do not develop neoplasia while isotype control 8–12 week group mice do. Percentage of the population with no dysplasia, LGD, HGD, and ACA is shown for each group (n = 8 per group).

(D and E) Treatment with anti-TNF-α does not ameliorate colitis or prevent the development of neoplasia in mice treated from 3 to 6 months. Histologic colitis score (y axis) and distribution of the degree of neoplasia (x axis) is shown (open circles, anti-TNF-α treated; shaded circles, isotype control treated). Each circle represents an individual mouse.

model (Rakoff-Nahoum et al., 2006) and in a carcinogen-treated *IL-10*$^{-/-}$ caCRC model (Uronis et al., 2009). Remarkably, *MyD88*$^{-/-}$ TRUC mice developed colitis of similar severity to TRUC (Figure 4B). Although these mice breed poorly and are severely immunocompromised, we generated five *MyD88*$^{-/-}$ TRUC mice that survived until 3 months of age. One of the five mice had submucosal ACA and 3/5 had dysplasia (Figure 4C). Thus, both inflammation and neoplasia in TRUC appear independent of *MyD88*, suggesting that classical TLR pathways are not necessary for TRUC caCRC.

We had previously shown that treating TRUC mice from 4–8 or 8–12 weeks of age with anti-TNF-α neutralizing antibody cured them of their microbe-driven inflammatory colitis. When mice were treated from 4–8 weeks with anti-TNF-α or isotype control antibody, no dysplasia was observed in either group, consistent with the limited exposure of the epithelium to an inflammatory milieu. However, 2/8 mice from the isotype control treated 8–12 week group had LGD and 1/8 mice had HGD, similar to the prevalence of neoplastic lesions we observed above (Figure 1). In contrast, none of the eight mice treated with anti-TNF-α antibody from 8–12 weeks developed dysplasia (Figure 4D). In recognition of published results that anti-TNF-α prevented dysplasia and carcinoma in the dextran sulfate sodium (DSS)/azoxymethane (AOM) caCRC model even when administered at late time points well after ACA has developed, we attempted to treat TRUC mice from 3 to 6 months of age (Popivanova

et al., 2008). We had high mortality (60%–75%) in both control treated and anti-TNF-α-treated cohorts and the four mice displayed for each group represent survivors of three independent experiments. Treatment with anti-TNF-α from 3 to 6 months of age had no effect on colitis and both the treatment and control groups had the same number of mice with HGD and ACA (Figure 4E). Although this small number of animals precludes a robust interrogation into the differences of the neoplastic microenvironment in the setting of this intervention, we did observe modest differences in several cytokines (IL-1β, IL-6, and IL-18) between anti-TNF and control treated mice (Figure S1C). Thus the commensal microflora and TNF-α are central initiators of caCRC, but delayed TNF-α neutralization is ineffective in halting neoplastic progression because it is unable to extinguish inflammation at this later stage.

TRUC and TRUC-Associated CRC Is Driven by Dendritic Cells and Can Be Prevented by Targeted Reexpression of *T-bet* in DCs

Innate immune cells play a key role in chronic inflammatory responses and much attention has been focused on macrophages and mast cells as inciters of the neoplastic environment (Bui and Schreiber, 2007; de Visser et al., 2006; Johansson et al., 2008). *T-bet* is not expressed, however, in macrophages or mast cells (L.H.G., unpublished data; Alcaide et al., 2007). Our previous work on the TRUC model suggested that T-bet functioned as a repressor of TNF-α in dendritic cells (DCs), but did not establish that DCs were necessary and sufficient for TRUC colitis. Two approaches were taken to determine the function of *T-bet* expressing DCs. In the first approach, we used the CD11c *diphtheria toxin receptor* (*DTR*) transgene to delete DCs in TRUC mice. TRUC mice expressing the CD11c *DTR* transgene were generated and then served as donors in bone marrow chimera experiments with TRUC mice as the recipients. After engraftment (8 weeks), we treated TRUC mice with diphtheria toxin every other day for 8 weeks to delete their DCs. Although the diphtheria treatment was toxic (~40% of the treatment cohort died), DC-depleted mice that did survive the treatment showed no evidence of colitis, whereas controls (TRUC into TRUC chimeras and PBS-treated CD11c *DTR* TRUC chimeras) had colitis (Figure 5A, left panel). As expected, diphtheria toxin treatment of transgenic bone marrow chimeric mice resulted in diminished colonic CD11c+ populations documented by indirect immunofluorescence microscopy (Figure 5A, right panel). Thus TRUC colitis appears dependent on DCs.

A second complementary approach addressed whether restoration of *T-bet* expression in DCs would ameliorate colitis and hence prevent neoplasia. We generated TRUC mice that overexpressed *T-bet* under the control of the *CD11c* promoter and verified expression in CD11c+ subsets from the colon and spleen of the transgenic TRUC mice (Figure 5B). Our previous published work, using primarily in vitro methodology, suggested that T-bet functioned as a repressor of TNF-α in DCs. The CD11c *T-bet* Tg TRUC had markedly reduced TNF-α levels in colonic explant cultures performed on mice at 4 weeks of age, suggesting that T-bet functions as a repressor in DCs in vivo (Figure 5C). Expression of *T-bet* did vary across the transgenic founders generated and we found that there was an inverse correlation between *T-bet* overexpression and colitis score in the CD11c *T-bet* Tg TRUC adult progeny of these founders (Figure 5 D). We set aside a cohort of mice for 6 months to observe the effects of *T-bet* overexpression in DCs on the development of inflammation and neoplasia. As shown in Figure 5E, (25/36) transgenics had no dysplasia versus (3/48) controls, (4/36) transgenics had HGD versus (12/48) controls, and (3/35) transgenics had ACA versus (30/48) controls. The difference between the number of nonneoplastic and neoplastic cases observed was statistically significant ($p < 0.0001$) between the CD11c *T-bet* transgenic TRUC and control TRUC. These data establish that DCs are critical for chronic inflammation in TRUC mice and that overexpression of *T-bet* in DCs rescues TRUC from dysplasia and cancer.

DISCUSSION

Inflammation is a key contributor to carcinogenesis and chronic inflammatory diseases, like IBD, initiate complex pathways to neoplasia. Here we report on a model of inflammation-driven colonic neoplasia dependent on the transcription factor T-bet and explore its similarity to human caCRC. TRUC mice provide unique opportunities to understand the role of innate immunity-driven inflammation and DCs in caCRC. Despite the intricacy of the inflammatory environment, selectively targeting one cell type, the DC, ablated inflammation in TRUC colons. Notably, selective, targeted overexpression of *T-bet* to DCs also substantially reduced neoplasia. Although initially discovered as the key regulator for CD4+ T helper type 1 T cell differentiation, T-bet has subsequently been found to have important functions in immune cell types spanning both the adaptive and innate immune system (Glimcher, 2007). Our group has previously examined the role of T-bet in the TRAMP prostate cancer and B16 melanoma models and defined a role for T-bet in limiting metastasis in TRAMP mice and more specifically mediating NK cell control of metastasis in the B16 model (Peng et al., 2004; Werneck et al., 2008). *T-bet* expression in CRC correlates with increased patient survival and decreased lymphovascular invasion within the tumor itself (Pages et al., 2005). *T-bet* expression in patient CRC samples is protective and, while expression has understandably been attributed to admixed T cells, our data that *T-bet* overexpression in DCs blunts colonic inflammation and reduces colonic neoplasia raise interest in the idea that *T-bet* expression in DCs may also play a protective role in patients as well. Transcription factor targeting has proven elusive as a cancer therapeutic; however, small molecule microarray-based assays and integrin antibody-targeted nanoparticles have made engineering therapeutics for altering *T-bet* expression in colonic DCs an achievable therapy for patients (Peer et al., 2008; Vegas et al., 2008).

IBD-driven CRC represents one extreme of how chronic inflammation shapes a proneoplastic environment. Proinflammatory cytokines, such as TNF-α, orchestrate effective defensive mechanisms against pathogens that can become inherently self-destructive in the acute setting of sepsis, pathogenic when triggered in response to the commensal microbiota or cross-reactive self-antigens in IBD and rheumatoid arthritis, or prometastatic in the subclinical inflammation present in numerous solid tumors (Smith, 2009). TNF was originally characterized by Lloyd Old in 1975 as a factor secreted by macrophages that killed the L-929 fibrosarcoma cell line (Old, 1988). Recombinant TNF-α is

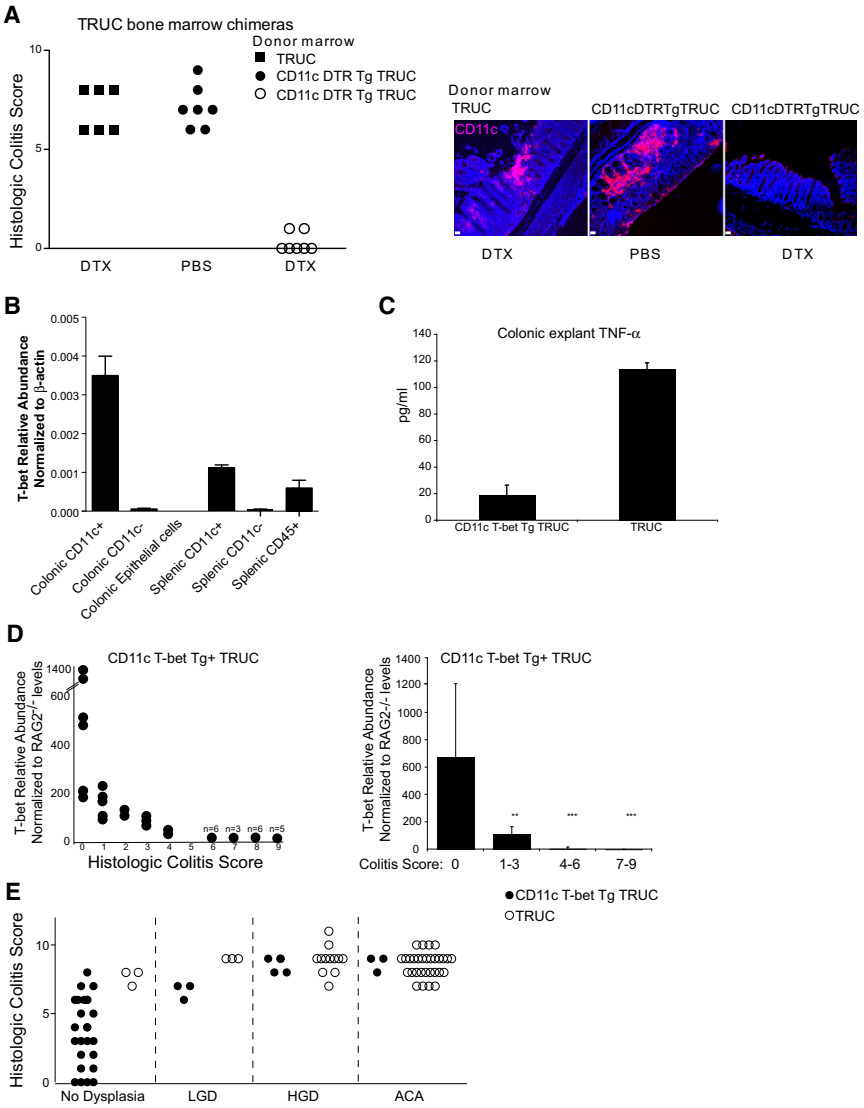

Figure 5. TRUC Colitis Is Dependent on DCs and *T-bet* Overexpression in DCs Reduces the Prevalence of TRUC Colitis-Associated Dysplasia and CRC

(A) TRUC colitis is dependent on DCs. CD11c DTR Tg+ TRUC mice were generated and used as donors in bone marrow chimera experiments with TRUC mice as recipients, TRUC bone marrow was engrafted into irradiated TRUC recipients as a control. After engraftment (8 weeks), CD11c DTR Tg+ TRUC chimeric mice were treated every other day with PBS (shaded circles) or DTX (open circles) for 8 weeks (left panel). Control TRUC bone marrow chimeras were DTX treated for 8 weeks (shaded squares) (left panel). Each dot represents one mouse. 40% of the original DTX-treated cohort group died during the 8 week course of treatment. Deletion of CD11c+ DC subsets was confirmed by indirect immunofluorescence microscopy for CD11c on paraffin-embedded sections from representative mice from each group. A selected image from the distal colon is shown for each group. CD11c, pink; Hoescht, blue. Scale bars, 50 μm.

(B) *T-bet* expression in CD11c *T-bet* Tg+ TRUC mice. *T-bet* expression was measured in purified myeloid colonic cell populations, in CEC populations, and in splenic cell populations pooled from 15 sex-matched CD11c *T-bet* Tg+ TRUC mice without evidence of colitis, using real-time qPCR. Bars represent the mean values across three replicate qPCR reactions on the samples and error bars ± SD.

(C) Restoration of *T-bet* expression using a CD11c transgenic cassette reduces colonic explant TNF-α levels in transgene expressing TRUC mice. TNF-α ELISA-based protein determinations from colonic explants from CD11c *T-bet* Tg+ TRUC and TRUC, age 4 weeks. Bars represent the mean value across three sets of explant samples (five individual mice per group) and error bars ± SD.

(D) *T-bet* overexpression inversely correlates with colitis score. qPCR for *T-bet* expression was performed on cDNA generated from RNA isolated from paraffin embedded CD11c *T-bet* Tg+ TRUC colons and *RAG2*$^{-/-}$ controls. T-bet abundance relative to β-actin and then normalized to *RAG2*$^{-/-}$ levels (y axis) is plotted versus colitis score (x axis). (left panel) Individual mice depicted by dots (when overlapping, the number of mice is shown above the dot). (right panel) Bars represent the mean values for mice grouped by colitis score (0, 1–3, 4–6, and 7–9) and error bars represent ± SD.

(E) CD11c *T-bet* Tg+ TRUC mice have reduced prevalence of dysplasia and carcinoma. Cohorts were aged to 6 months and evaluated for colitis (y axis) and neoplasia (grouped by histopathology along the x axis), CD11c *T-bet* Tg+ TRUC (shaded circles, n = 35), and control TRUC (open circles, n = 48).

currently in clinical trials for ovarian and head and neck cancer as well as a number of advanced solid tumors (http://www.cancer.gov/clinicaltrials). However, TNF-α also may be a culprit in driving metastasis as recently suggested by the observations that TNF-α stabilizes Snail via NF-κB activation of the COP9 signalosome2 and that knockdown of Snail inhibited inflammation-driven breast cancer metastasis (Wu et al., 2009). Clearly, the relationship between TNF-α and cancer is complex as highlighted here. We have previously demonstrated that T-bet functions as a repressor of TNF-α in DCs and that TNF-α neutralization can both ameliorate and block colitis at its inception and cure established colitis. Nevertheless, there appear to be therapeutic limits to TNF-α blockade in preventing neoplasia in TRUC, as neutralization from 3–6 months of age did not prevent HGD and ACA. This observation is in contrast to recent findings in the DSS/AOM model of caCRC, where late stage CRC was successfully treated with TNF blockade (Popivanova et al., 2008). We have previously shown that TRUC CECs cultured ex vivo demonstrate an increased sensitivity to TNF-α-induced cell death. However, the cell death and proliferation experiments in conjunction with the TNF-α colon explant ELISA data suggest that TRUC CECs may reprogram this sensitivity to TNF-α-induced cell death. Our studies of TRUC mice, a spontaneous model of caCRC, suggest that TNF-α in a chronically inflamed mucosa may initiate a cascade of events that engender dysplasia and cancer. However, once this process is unleashed neither blockade of TNF-α nor excess TNF-α is effective in halting neoplastic progression.

While TNF is a key effector in both IBD and inflammation-driven cancer, other proinflammatory cytokines play central roles as well. Pleiotropic protumorigenic effects have been ascribed to IL-6 in a number of epithelial cancers (colon, breast, lung, and liver) (Lin and Karin, 2007). More recently, IL-6 has been shown to be critical for the development of caCRC via its antiapoptotic effects and induction of hypoxia genes via the IL-6 downstream effector STAT3 in the colonic epithelium (Grivennikov et al., 2009). Furthermore, carcinoma-produced factors are adept at eliciting high levels of host myeloid IL-6 and TNF-α (Kim et al., 2009). IL-1β, like TNF-α, can initiate proinflammatory cascades driving the production of proinflammatory mediators (COX-2 and iNOS), cytokines (IL-6), growth factors, adhesion molecules, and matrix metalloproteinases. Numerous cytokines trigger mediators aimed at the resolution phase of injury and these growth factors and proteases may be construed as healing. However, in a chronically inflamed mucosa the epithelium is altered and compromised in appropriate signal processing. In our experiments, we show clear evidence of aneuploidy, ROS, and DNA adducts prior to the histologic diagnosis of dysplasia or cancer. The importance of DNA repair mechanisms in response to reactive oxygen and nitrogen species-induced DNA damage was elegantly demonstrated in the setting of alkyladenine DNA glycosylase (a major DNA repair enzyme) deficiency in inducible mouse models of gastritis and colon cancer (Meira et al., 2008). A model put forth in that study emphasizes both the importance of proinflammatory effectors and epithelial cells with DNA alterations for inflammatory-associated neoplasia. While cytokines, inflammatory mediators, and DNA damage may all be essential for caCRC, the inciting event rests in the host's response to the commensal microbiota.

There is a growing appreciation for host-commensal interrelationships in colon cancer. Genetic deletion of *TLR4*, which signals through MyD88, protects mice from CaCRC induced by DSS/AOM. Several patients with CaCRC have increased *TLR4* epithelial expression and AOM-induced CRC in *IL-10*$^{-/-}$ mice is commensal and *MyD88* dependent (Fukata et al., 2007; Uronis et al., 2009). The innate immune adaptor molecule MyD88 controls the expression of many epithelial genes influencing tumor development in the *APC/min-* mouse model and in carcinogen (AOM)-induced colon cancer (Rakoff-Nahoum and Medzhitov, 2007). However, our results that TRUC colitis and caCRC are *MyD88* independent suggest that not all caCRC is dependent on *MyD88*. Commensal microbial signals may act via TLR pathways that signal to NF-κB through TRIF or non-TLR pathways, driven by glycan-based PAMPs that bind C-type lectin receptors and activate Syk, resulting in NF-κB activation via Card9, as is the case for Dectin-1 (Ruland, 2008), or via intracellular bacterial-derived products that activate the NOD1/2 pathway. Identification of the microbes driving inflammation in TRUC will hopefully inform our understanding of the pathogen recognition receptor pathways they trigger.

Our experiments provide insight into the role of T-bet and the innate immune system in colon cancer. We show that a complex and proneoplastic inflammatory environment can be ablated by deletion of DCs. Furthermore, we demonstrate that overexpression of the transcription factor *T-bet* rescues colitic mice from caCRC. In conclusion, we present a robust model of caCRC that provides insight into both disease pathogenesis and therapeutic approaches and also furnishes ample opportunities for basic scientific discovery and preclinical testing.

EXPERIMENTAL PROCEDURES

Generation of TRUC Mice and CD11c *T-bet* IRES *eGFP* Tg *T-bet*$^{-/-}$ × *RAG2*$^{-/-}$ Mice

Mice were housed in microisolator cages in the barrier facility of the Harvard School of Public Health. Animal studies and experiments were approved and carried out according to Harvard University's Standing Committee on Animals and National Institutes of Health guidelines for animal use and care. Mice in the colony are specific pathogen free and are negative for *Helicobacter hepaticus*, *bilis*, and *muridarum*.

Mice with deletion of *T-bet* and *RAG2* and their genotyping have been described previously (Lugo-Villarino et al., 2005).

The CD11c expression cassette was generated in the laboratory of D. Littman and a *T-bet* IRES *eGFP* construct was subcloned into it. CD11c *T-bet* IRES *eGFP* transgenic mice were generated by injection of this linearized construct into *T-bet*$^{-/-}$ *RAG2*$^{-/-}$ deficient embryos and implanted into pseudo-pregnant TRUC mice to preserve the TRUC microbiota. Mice were genotyped for transgene expression using a modified protocol from the Jackson Laboratory. Primer sets were as follows: CTAGGCCACAGAATTGAAAG ATCT, GTAGGTGGAAATTCTAGCATCATCC, AAGTTCATCTGCACCACCG, and TCCTGAAGAAGATGGTGCG (GFP and endogenous IL-2).

Founder mice were screened for expression using flow cytometry for GFP fluorescence of CD11c+ subsets from blood, spleen, and colon. Mice were subsequently screened by real-time qPCR for *T-bet* expression from RNA isolated from spleen and colon cell subsets (generated using MACS selection) using the primers CAACAACCCCTTTGCCAAAG and TCCCCCAAGCAGTTG ACAGT.

T-bet$^{-/-}$ *RAG2*$^{-/-}$ were bred to the *MyD88*-deficient mice (obtained from the laboratory of D. Goldstein with permission from S. Akira).

Broad-Spectrum Antibiotic Treatment of TRUC Colitis

Mice were treated for 6 months with ampicillin (1 g/l; Roche), vancomycin (500 mg/l; Henry Schein, Inc. [Hospira, Inc.]), neomycin sulfate (1 g/l; Sigma [Teva Pharmaceuticals]), and metronidazole (1 g/l; Sigma; solubilized with 15 ml of 0.1 N acetic acid/liter) dissolved in their autoclaved drinking water acid and fluid intake was monitored.

Generation of CD11c *DTR GFP* TRUC Mice

CD11c *DTR eGFP* Tg mice from the Jackson Laboratory were crossed to *T-bet*$^{-/-}$ *RAG2*$^{-/-}$ mice and genotyped for presence of the transgene as per Jackson Laboratory protocol. High expressing mice (by analysis of CD11c+ GFP+ population from peripheral blood) were bred and selected as donors in bone marrow chimera experiments.

TRUC mice were irradiated with 800 rads and received CD11c *DTR eGFP* Tg+ TRUC or TRUC bone marrow 2 hr after irradiation. After engraftment (8 weeks), transgene expression was tested by peripheral blood flow cytometry and mice were treated with PBS or 10 ng/gm mouse weight of diphtheria toxin (Sigma) every other day for 8 weeks.

Histology

Colons were removed from mice after termination and dissected free from the anus to distal to the cecum. Colonic contents were removed and colons cleaned with PBS prior to fixation in 4% PFA or 10% neutral buffered formalin followed by routine paraffin embedding. After paraffin embedding, 0.5 μm sections were cut and stained with hematoxylin and eosin or as noted.

Sections were examined and colitis was scored in a blinded fashion (with respect to genotype and experimental protocol) by one of the authors (J.N.G.). Each of four histologic parameters was scored as absent (0), mild (1), moderate (2), or severe (3): mononuclear cell infiltration, polymorphonuclear cell infiltration, epithelial hyperplasia, and epithelial injury, similar to previous studies (Neurath et al., 2002). For cancer incidence studies, J.N.G. examined all tissues for dysplasia and CRC in a blinded fashion on two independent occasions. Assessment for dysplasia and cancer was based on the criteria set forth in the Mouse Models of Intestinal Cancers consensus report:

location, presence/absence of prolapse/herniation, size (in mm), dysplasia grade, invasion level, presence of desmoplasia, and presence of irregular architecture (gland crowding, solid nests of cells versus single cells, irregularity or cribiforming, presence of lateral spread, and loss of acini) (Boivin et al., 2003).

Immunohistochemistry

Paraffin-embedded colon sections were deparaffinized, rehydrated, and pretreated with hydrogen peroxidase in PBS buffer. Heat-induced antigen retrieval was performed.

After blocking with the appropriate antisera in blocking buffer, sections were incubated with anti-PCNA (1:100), anti-β-catenin (BD Biosciences clone 14/β-catenin; 1:900 dilution), anti-p53 (clone CM5 [1:400]), or anti-COX-2 (Santa Cruz clone c-20; 1:50 dilution) for 1 hr at room temperature. After incubation with HRP-conjugated secondary antibody and tyramide amplification followed by streptavidin-HRP, positive signals were visualized by DAB kit and counterstained with hematoxylin.

Quantitation

COX-2

Total crypts and COX-2+ crypts were scored from three TRUC mice with and three without neoplasia. Four lower power (10× objective), contiguous fields spanning the distal colons were scored.

p53

Total crypt number, number of crypts with p53 staining, and number of positive cells per crypt were quantitated across two low power (10× objective) fields spanning the distal colon for nine TRUC mice with and nine without carcinoma and dysplasia.

Isolation of RNA from Paraffin-Embedded Tissues

RNA was isolated from microdissected paraffin-embedded tissues using the RecoverAll Total Nucleic Acid Isolation Kit according to the manufacturer's instructions.

Generation of cDNA from RNA

cDNA was generated from isolated RNA using the Invitrogen iScript kit.

Real-Time qPCR

Real-time qPCR was carried out using ABI SyBR reagent on an ABI 7700 or Stratagene Mx3005p using SYBR or POWER SYBR green master mix from ABI. HPRT, unless otherwise noted, was the housekeeping gene used.

Primer Design

Unless otherwise noted, primers used were from validated sets designed by Primer Bank (http://pga.mgh.harvard.edu/primerbank/index.html).

BrDU Staining

Mice were injected with 200 μl BrDU i.p. and sacrificed after 2 hr. Colons were subsequently fixed for 2 hr in neutral-buffered formalin, placed in 70% EtOH overnight, embedded, and stained for BrDU using the BrDU detection kit from BD Biosciences. Sections were counterstained with DAPI and for assessment of cell death in conjunction with cell proliferation; sections were stained using the Roche TUNEL in situ death fluorescence kit.

Colonic Crypt Isolation

In brief, cells were isolated from cleaned minced colons using HBBS with 1 mM EDTA/1 mM EGTA as previously described (Garrett et al., 2007).

p53 Activity Assays

Colonic crypts were isolated as above from the distal colon of *RAG2*$^{-/-}$ mice or colitic or neoplastic segments of TRUC colons. CECs were treated with doxorubicin at 0.5 μg/ml for 8 hr or vehicle alone. Twenty segments were pooled per group to generate a sufficient number of cells for RNA isolation or nuclear extracts. Two separate isolations and treatments of the CECs were performed and data represent the mean ± SD across these groups. RNA was isolated and cDNA was generated as described. β-*Actin* was the housekeeping gene used for relative abundance calculations and a fold change was calculated for *p21* and *APAF1* induction relative to detection levels in control-treated samples. For DNA binding activity, nuclear extracts were generated as per the manufacturer's instructions for the Duoset IC intracellular human/mouse p53 activity assay with the exception that lysis buffers A and B were prepared with Roche protease and PhosSTOP inhibitor cocktail tablets and 20 μg of extract was used per well.

Aneuploidy Analysis

Colonic crypt cells were isolated and cells were then fixed in ice-cold ethanol at a final concentration of 70% using vigorous vortexing, RNase treated, stained with anti-CD45-APC antibody to exclude any myeloid contaminating subsets, and stained with propidium iodide. Data were acquired using a BD LSRII flow cytometer and the flow cytometer was calibrated for DNA ploidy analysis using the BD DNA QC particle kit. The HT-29 cell line was used as a positive control for aneuploid populations. Data were analyzed using ModFIT software (Clausen et al., 2001).

Measurement of Reactive Oxygen Species

Colons were removed after sacrifice and cleaned distal colons were divided into three segments and placed in a buffer of 1 mM $CaCl_2$ and 5 mM glucose. Colonic segments were weighed and then placed into luminol assay buffer (0.045 g luminol in PBS). After a 3 min incubation, luminescence was measured using a luminometer. The average across all segments constituted the value for each mouse. After weight correction, values were averaged for six to nine mice per time point (Millar et al., 1996).

Western Blots

CECs were isolated and lysates were generated using RIPA buffer in the presence of protease inhibitors. Protein lysates were resolved using SDS-PAGE and transferred to PVDF membrane using a Bio-Rad Wet transfer apparatus. Blots were probed with antibodies directed against Bcl-2, Bax, Bak, Bcl-xL, and Hsp90 (all from Santa Cruz Biotechnology, Inc.). After incubation with the appropriate HRP-conjugated secondary antibody, we used ECL to develop the blots.

Measurement of DNA Adducts

DNA was extracted from CECs from the distal colon using the QIAGEN genomic DNA extraction kit as per the manufacturer's protocol. Samples were processed as per the manufacturer's instructions for the high sensitivity 8-OHdG ELISA kit K0G-HS10E with the following exceptions. Nuclease P1 and alkaline phosphatase digestions were performed in an An02 hood. After processing, DNA-digested samples from six to nine mice per time point were pooled and subjected to quantitation by ELISA in triplicate.

Anticytokine Therapy

Anti-TNF-α (clone TN3-19.12), a hamster anti-mouse TNF-α neutralizing IgG1, and isotype control were a kind gift of R. Schreiber and purchased from Leinco Technologies, Inc. Fifteen micrograms per gram of mouse weight of antibody was injected i.p. every 7 days for durations as noted. Mice were sacrificed 1 week following the last injection.

Colon Explant Culture

Explant cultures were carried out following a modification of previously described procedures (Rakoff-Nahoum et al., 2004). One centimeter segments of the distal colon were washed in HBBS containing penicillin, streptomycin, and gentamicin. The segments were cultured in 48 well flat bottom plates with complete RPMI media supplemented with penicillin, streptomycin, and gentamicin. Media was collected after 4 hr and centrifuged to remove debris. After centrifugation, the supernatant was aliquoted and stored at −80C.

Measurement of Cytokines

Cytokines were measured in culture supernatants utilizing SearchLight high dynamic range imaging and analysis unless otherwise indicated. For IL-10 and TNF-α, the mouse OptEIA ELISA kit (BD Biosciences) was used as per the manufacturer's instructions.

Statistical Analysis

Statistical analyses were performed using the Mann-Whitney U nonparametric test for ordinal data. Error bars represent ± SD unless otherwise noted.

SUPPLEMENTAL DATA

Supplemental Data include one figure and can be found with this article online at http://www.cell.com/cancer-cell/supplemental/S1535-6108(09)00250-5.

ACKNOWLEDGMENTS

We thank Jacobo Ramirez and Diana Pascual for outstanding care of our mice; Landy Kangaloo and members of the Glimcher laboratory for helpful discussion; Drs. Vanja Lazarevic, Marc Wein, Fabio Martinon, and Tracy Staton for critical review of the manuscript; and Drs. Tyler Jacks, Ji-Hye Paik, and Alfred Zullo for advice. This work was supported by grants from the National Institutes of Health (CA112663) and an Ellison Scholar Award to L.H.G. W.S.G. is a recipient of a Damon Runyon Cancer Research Foundation fellowship, a Burroughs Wellcome Career in Medical Sciences Award, and funding from the V Foundation, DF/HCC GI SPORE 1P50CA127003-02, Irving Janock Fellowship, and HDDC Pilot Award. L.H.G. holds equity and is on the Board of Directors of Bristol-Myers Squibb. Dedicated in memory of R.B., L.K., and N.H., whose battles with CRC were an inspiration for this study.

Received: March 11, 2009
Revised: May 29, 2009
Accepted: July 22, 2009
Published: September 8, 2009

REFERENCES

Agoff, S.N., Brentnall, T.A., Crispin, D.A., Taylor, S.L., Raaka, S., Haggitt, R.C., Reed, M.W., Afonina, I.A., Rabinovitch, P.S., Stevens, A.C., et al. (2000). The role of cyclooxygenase 2 in ulcerative colitis-associated neoplasia. Am. J. Pathol. *157*, 737–745.

Alcaide, P., Jones, T.G., Lord, G.M., Glimcher, L.H., Hallgren, J., Arinobu, Y., Akashi, K., Paterson, A.M., Gurish, M.A., and Luscinskas, F.W. (2007). Dendritic cell expression of the transcription factor T-bet regulates mast cell progenitor homing to mucosal tissue. J. Exp. Med. *204*, 431–439.

Berg, D.J., Davidson, N., Kuhn, R., Muller, W., Menon, S., Holland, G., Thompson-Snipes, L., Leach, M.W., and Rennick, D. (1996). Enterocolitis and colon cancer in interleukin-10-deficient mice are associated with aberrant cytokine production and CD4(+) TH1-like responses. J. Clin. Invest. *98*, 1010–1020.

Boivin, G.P., Washington, K., Yang, K., Ward, J.M., Pretlow, T.P., Russell, R., Besselsen, D.G., Godfrey, V.L., Doetschman, T., Dove, W.F., et al. (2003). Pathology of mouse models of intestinal cancer: consensus report and recommendations. Gastroenterology *124*, 762–777.

Bui, J.D., and Schreiber, R.D. (2007). Cancer immunosurveillance, immunoediting and inflammation: independent or interdependent processes? Curr. Opin. Immunol. *19*, 203–208.

Cho, K.R., and Vogelstein, B. (1992). Genetic alterations in the adenoma–carcinoma sequence. Cancer *70*, 1727–1731.

Clausen, O.P., Andersen, S.N., Stroomkjaer, H., Nielsen, V., Rognum, T.O., Bolund, L., and Koolvraa, S. (2001). A strategy combining flow sorting and comparative genomic hybridization for studying genetic aberrations at different stages of colorectal tumorigenesis in ulcerative colitis. Cytometry *43*, 46–54.

D'Inca, R., Cardin, R., Benazzato, L., Angriman, I., Martines, D., and Sturniolo, G.C. (2004). Oxidative DNA damage in the mucosa of ulcerative colitis increases with disease duration and dysplasia. Inflamm. Bowel Dis. *10*, 23–27.

de Visser, K.E., Eichten, A., and Coussens, L.M. (2006). Paradoxical roles of the immune system during cancer development. Nat. Rev. Cancer *6*, 24–37.

Dianda, L., Hanby, A.M., Wright, N.A., Sebesteny, A., Hayday, A.C., and Owen, M.J. (1997). T cell receptor-alpha beta-deficient mice fail to develop colitis in the absence of a microbial environment. Am. J. Pathol. *150*, 91–97.

Eaden, J.A., Abrams, K.R., and Mayberry, J.F. (2001). The risk of colorectal cancer in ulcerative colitis: a meta-analysis. Gut *48*, 526–535.

Fukata, M., Chen, A., Vamadevan, A.S., Cohen, J., Breglio, K., Krishnareddy, S., Hsu, D., Xu, R., Harpaz, N., Dannenberg, A.J., et al. (2007). Toll-like receptor-4 promotes the development of colitis-associated colorectal tumors. Gastroenterology *133*, 1869–1881.

Garrett, W.S., Lord, G.M., Punit, S., Lugo-Villarino, G., Mazmanian, S.K., Ito, S., Glickman, J.N., and Glimcher, L.H. (2007). Communicable ulcerative colitis induced by T-bet deficiency in the innate immune system. Cell *131*, 33–45.

Glimcher, L.H. (2007). Trawling for treasure: tales of T-bet. Nat. Immunol. *8*, 448–450.

Grivennikov, S., Karin, E., Terzic, J., Mucida, D., Yu, G.Y., Vallabhapurapu, S., Scheller, J., Rose-John, S., Cheroutre, H., Eckmann, L., and Karin, M. (2009). IL-6 and Stat3 are required for survival of intestinal epithelial cells and development of colitis-associated cancer. Cancer Cell *15*, 103–113.

Itzkowitz, S. (2003). Colon carcinogenesis in inflammatory bowel disease: applying molecular genetics to clinical practice. J. Clin. Gastroenterol. *36*, S70–S74; discussion S94–S96.

Johansson, M., Denardo, D.G., and Coussens, L.M. (2008). Polarized immune responses differentially regulate cancer development. Immunol. Rev. *222*, 145–154.

Kim, S., Takahashi, H., Lind, W.W., Descargues, P., Grivennikov, S., Kim, Y., Luo, J.L., and Karin, M. (2009). Carcinoma-produced factors activate myeloid cells through TLR2 to stimulate metastasis. Nature *457*, 102–106.

Lacy-Hulbert, A., Smith, A.M., Tissire, H., Barry, M., Crowley, D., Bronson, R.T., Roes, J.T., Savill, J.S., and Hynes, R.O. (2007). Ulcerative colitis and autoimmunity induced by loss of myeloid alphav integrins. Proc. Natl. Acad. Sci. USA *104*, 15823–15828.

Lin, W.W., and Karin, M. (2007). A cytokine-mediated link between innate immunity, inflammation, and cancer. J. Clin. Invest. *117*, 1175–1183.

Lugo-Villarino, G., Ito, S., Klinman, D.M., and Glimcher, L.H. (2005). The adjuvant activity of CpG DNA requires T-bet expression in dendritic cells. Proc. Natl. Acad. Sci. USA *102*, 13248–13253.

Ma, A. (2007). Loss of T-bet sends host-microbe mutualism awry. Cell *131*, 15–17.

Meira, L.B., Bugni, J.M., Green, S.L., Lee, C.W., Pang, B., Borenshtein, D., Rickman, B.H., Rogers, A.B., Moroski-Erkul, C.A., McFaline, J.L., et al. (2008). DNA damage induced by chronic inflammation contributes to colon carcinogenesis in mice. J. Clin. Invest. *118*, 2516–2525.

Meling, G.I., Clausen, O.P., Bergan, A., Schjolberg, A., and Rognum, T.O. (1991a). Flow cytometric DNA ploidy pattern in dysplastic mucosa, and in primary and metastatic carcinomas in patients with longstanding ulcerative colitis. Br. J. Cancer *64*, 339–344.

Meling, G.I., Rognum, T.O., Clausen, O.P., Chen, Y., Lunde, O.C., Schlichting, E., Wiig, J.N., Hognestad, J., Bakka, A., Havig, O., et al. (1991b). Association between DNA ploidy pattern and cellular atypia in colorectal carcinomas. A new clinical application of DNA flow cytometric study? Cancer *67*, 1642–1649.

Millar, A.D., Rampton, D.S., Chander, C.L., Claxson, A.W., Blades, S., Coumbe, A., Panetta, J., Morris, C.J., and Blake, D.R. (1996). Evaluating the antioxidant potential of new treatments for inflammatory bowel disease using a rat model of colitis. Gut *39*, 407–415.

Neurath, M.F., Weigmann, B., Finotto, S., Glickman, J., Nieuwenhuis, E., Iijima, H., Mizoguchi, A., Mizoguchi, E., Mudter, J., Galle, P.R., et al. (2002). The transcription factor T-bet regulates mucosal T cell activation in experimental colitis and Crohn's disease. J. Exp. Med. *195*, 1129–1143.

Old, L.J. (1988). Tumor necrosis factor. Sci. Am. *258*, 59–60, 69–75.

Pages, F., Berger, A., Camus, M., Sanchez-Cabo, F., Costes, A., Molidor, R., Mlecnik, B., Kirilovsky, A., Nilsson, M., Damotte, D., et al. (2005). Effector memory T cells, early metastasis, and survival in colorectal cancer. N. Engl. J. Med. *353*, 2654–2666.

Peer, D., Park, E.J., Morishita, Y., Carman, C.V., and Shimaoka, M. (2008). Systemic leukocyte-directed siRNA delivery revealing cyclin D1 as an anti-inflammatory target. Science *319*, 627–630.

Peng, S.L., Townsend, M.J., Hecht, J.L., White, I.A., and Glimcher, L.H. (2004). T-bet regulates metastasis rate in a murine model of primary prostate cancer. Cancer Res. *64*, 452–455.

Popivanova, B.K., Kitamura, K., Wu, Y., Kondo, T., Kagaya, T., Kaneko, S., Oshima, M., Fujii, C., and Mukaida, N. (2008). Blocking TNF-alpha in mice

reduces colorectal carcinogenesis associated with chronic colitis. J. Clin. Invest. *118*, 560–570.

Rakoff-Nahoum, S., and Medzhitov, R. (2007). Regulation of spontaneous intestinal tumorigenesis through the adaptor protein MyD88. Science *317*, 124–127.

Rakoff-Nahoum, S., and Medzhitov, R. (2009). Toll-like receptors and cancer. Nat. Rev. Cancer *9*, 57–63.

Rakoff-Nahoum, S., Paglino, J., Eslami-Varzaneh, F., Edberg, S., and Medzhitov, R. (2004). Recognition of commensal microflora by toll-like receptors is required for intestinal homeostasis. Cell *118*, 229–241.

Rakoff-Nahoum, S., Hao, L., and Medzhitov, R. (2006). Role of toll-like receptors in spontaneous commensal-dependent colitis. Immunity *25*, 319–329.

Ravizza, R., Gariboldi, M., Passarelli, L., and Monti, E. (2004). Role of the p53/p21 system in the response of human colon carcinoma cells to Doxorubicin. BMC Cancer *4*, 92.

Rodrigues, N.R., Rowan, A., Smith, M.E.F., Kerr, I.B., Bodmer, W.F., Gannon, J.V., and Lane, D.P. (1990). p53 mutations in colorectal cancer. Proc. Natl. Acad. Sci. USA *87*, 7555–7559.

Rubin, C.E., Haggitt, R.C., Burmer, G.C., Brentnall, T.A., Stevens, A.C., Levine, D.S., Dean, P.J., Kimmey, M., Perera, D.R., and Rabinovitch, P.S. (1992). DNA aneuploidy in colonic biopsies predicts future development of dysplasia in ulcerative colitis. Gastroenterology *103*, 1611–1620.

Rudolph, U., Finegold, M.J., Rich, S.S., Harriman, G.R., Srinivasan, Y., Brabet, P., Bradley, A., and Birnbaumer, L. (1995). Gi2 alpha protein deficiency: a model of inflammatory bowel disease. J. Clin. Immunol. *15*, 101S–105S.

Ruland, J. (2008). CARD9 signaling in the innate immune response. Ann. NY Acad. Sci. *1143*, 35–44.

Shah, S.A., Simpson, S.J., Brown, L.F., Comiskey, M., de Jong, Y.P., Allen, D., and Terhorst, C. (1998). Development of colonic adenocarcinomas in a mouse model of ulcerative colitis. Inflamm. Bowel Dis. *4*, 196–202.

Smith, O.M. (2009). Immunology select. Cell *137*, 591–593.

Uronis, J.M., Muhlbauer, M., Herfarth, H.N., Rubinas, T.C., Jones, G.S., and Jobin, C. (2009). Modulation of intestinal microbiota alters colitis-associated colorectal susceptibility. PLoS ONE *4*, e6026.

Vegas, A.J., Fuller, J.H., and Koehler, A.N. (2008). Small-molecule microarrays as tools in ligand discovery. Chem. Soc. Rev. *37*, 1385–1394.

Werneck, M.B., Lugo-Villarino, G., Hwang, E.S., Cantor, H., and Glimcher, L.H. (2008). T-bet plays a key role in NK-mediated control of melanoma metastatic disease. J. Immunol. *180*, 8004–8010.

Wu, Y., Deng, J., Rychahou, P.G., Oiu, S., Evers, B.M., and Zhou, B.P. (2009). Stabilization of snail by NF-kappaB is required for inflammation-induced cell migration and invasion. Cancer Cell *15*, 416–428.

Xie, J., and Itzkowitz, S.H. (2008). Cancer in inflammatory bowel disease. World J. Gastroenterol. *14*, 378–389.

Yoshida, T., Mikami, T., Mitomi, H., and Okayasu, I. (2003). Diverse p53 alterations in ulcerative colitis-associated low-grade dysplasia: full-length gene sequencing in microdissected single crypts. J. Pathol. *199*, 166–175.